FIRST OBSERVATIONS WITH THE EFFELSBERG RADIO TELESCOPE AT 7-MM WAVELENGTH. II. A SURVEY OF STARS IN THE VIBRATIONALLY EXCITED $J = 1$–0 SiO LINES

J. H. SPENCER
E. O. Hulburt Center for Space Research, Naval Research Laboratory, Washington, D.C. 20375

A. WINNBERG
Max-Planck-Institut für Radioastronomie, Auf dem Hügel 69, D-5300 Bonn 1, West Germany

F. M. OLNON
Sterrewacht-Huygens Laboratorium, Wassenaarsweg 78, Leiden 2405, The Netherlands

P. R. SCHWARTZ
E. O. Hulburt Center for Space Research, Naval Research Laboratory, Washington, D.C. 20375

H. E. MATTHEWS
Herzberg Institute of Astrophysics, National Research Council, Ottawa, Ontario K1A 0R6, Canada

D. DOWNES
Institut de Radio Astronomie Millimetrique, B.P. 391, 38017 Grenoble, France
Received 14 October 1980; revised 24 November 1980

ABSTRACT

High-resolution and high-sensitivity spectra are presented for 46 SiO masers in the $J = 1$–0 transitions of the $v = 1$, $v = 2$, and $v = 3$ excited states. The emission is a complex blend of weak maser lines. Our sample is statistically complete to a distance of approximately 300 pc, but is sensitivity limited. The luminosity functions are the same for $v = 1$ and $v = 2$ regardless of their shape, but the $v = 1$ line is, on the average, 1.4 times stronger than the $v = 2$ line in the same star. A luminosity function corrected for incompleteness has been obtained using a new method. The SiO luminosity is not correlated with other stellar properties, which indicates that local conditions in the stellar atmospheres determine the maser intensity.

I. INTRODUCTION

SiO masers provide important information on the physical conditions in circumstellar shells and the mechanisms of mass loss. Visual and infrared observations limit possible models of these stellar masers more than for masers in regions of star formation. The SiO maser remains unique in that it is found only in late-type stars, with the possible exception of the source IRc 2 in Orion (Genzel *et al.* 1980). Because of their large distance and complexity, late-type stars are not as well understood as other types of stars. Many of their known properties are derived from statistical techniques. With the number of SiO masers now known, it is possible to do statistical studies to derive some of the physical properties of these stars.

A high-sensitivity survey of 7-mm SiO lines of a large number of stars, conducted within a short time (~1 month), can be used to test for correlations between the maser intensity and parameters of the stellar envelopes. Nearly simultaneous observations at different vibrational states limit uncertainties due to maser variations in these maser model tests.

In the spring of 1979 the 100-m radio telescope in Effelsberg became available for 7-mm observations and a survey of this type was attempted. In this paper we report the results of the observations of the vibrationally excited $J = 1$–0 SiO lines. A separate paper on the ground-state $v = 0$ observations of these stars is in preparation.

II. OBSERVATIONS

The receiver and telescope characteristics have been described by Altenhoff *et al.* (1980, hereafter referred to as Paper I). The observations were taken in a total-power on-off mode with total on-source integration times of 5 to 10 min. Individual on-source components of this integration time were between 1 and 3 min. The E vector of polarization was vertical, producing a rotation of the position angle of the E vector as the source was tracked across the sky.

 0004-6256/81/030392-18$00.90

Most of the spectra reported here were taken with an autocorrelator, with spectral resolutions of 62.5 or 31.3 kHz (~0.44 or ~0.22 km s^{-1}) and a total bandwidth of 10 or 5 MHz, respectively. The $v = 1$ and $v = 2$ lines were observed simultaneously in the two parts of the autocorrelator with 192 channels for each. We also used a filter spectrometer consisting of 128 filters with widths of 312.5 kHz (~2.2 km s^{-1}). These filters were shared between either $v = 1$ and $v = 2$, or $v = 0$ and $v = 3$, to give an effective filter spectrometer of 50 to 65 filters with a velocity range of 105 to 140 km s^{-1}. In addition to the spectra presented in this paper, we observed several of the strong SiO masers with the filter spectrometer.

Because the number of known SiO masers was not statistically large, the present observations included many stars that were not known to have SiO maser emission in an attempt to increase the number of known masers.

The selection criteria for the search for new SiO masers included:

(1) Mira variables from Keenan *et al.* (1974) with $m - M < 9.8^m$ (corresponding to $D < 900$ pc) and with $\delta > -10°$.

(2) IRC sources (Neugebauer and Leighton 1969) with $K \leq 2$ and $I - K \geq 5$ and with $\delta > -10°$.

(3) Stars known to have associated masers (either OH, H_2O, or SiO) (cf. Kleinmann *et al.* 1978 or Engels 1979).

(4) CRL sources with photometry and good positions (Low *et al.* 1976).

(5) Peculiar stars such as P Cyg or MWC 349.

We also included some pre-main-sequence stars like T Tauri stars and M supergiants like α Ori that do not fit any of these criteria exactly. The results of observations on early-type stars and regions of star formation are discussed in Genzel *et al.* (1980). Until the mechanisms of masers associated with stars are better understood, these objects will continue to be included in the observing lists, thus making them statistically incomplete and contaminated.

Except for the unusual object IRC+10216, the list of stars to search for $v = 3$ emission was composed from the list of known SiO $v = 1$ and $v = 2$ emission stars. In the case of IRC+10216 (= CW Leo) the $v = 3$ search was conducted for technical reasons as part of the principal $v = 0$ search. The amount of time spent searching a star for $v = 3$ was determined as much by observing pressure as by *a priori* expectations.

III. RESULTS

The results are listed in Tables I–III. Stars with a positive detection in either the $v = 1$ or $v = 2$ transition are to be found in Table I. The spectra of these stars are presented in Figs. 1–8. The name of the star is given in column 1, with the IRC number in column 2. The distances (column 3 of Table I) are derived from the mass, luminosity, period, and spectral type at maximum (Cahn and Wyatt 1978; Cahn 1980). Stars that are not Miras or do not fit the Cahn and Wyatt criteria were estimated by other techniques as noted. Some distances were calculated from the relation between period and absolute visual magnitude M_v at mean maximum as given by Foy *et al.* (1975). The interstellar absorption A_v was estimated from an assumed extinction law:

$$A_v = 0.14 \csc b [1 - \exp(-0.01 d \sin b)], \quad (1)$$

where d is the distance in parsecs and b is the galactic latitude. Further, stars whose distances were calculated in this manner were rarely used in the detailed analysis of Sec. IV. Distances for supergiants and some infrared stars are from Hyland *et al.* (1972), except for VY CMa and S Per. The Herbig (1969) distance of 1500 pc was adopted for VY CMa, while S Per was assumed to be associated with the h and χ Per clusters (Kukarkin *et al.* 1969–1976). The phase of the optical light cycle is listed in column 4 of Table I. Columns 5 and 6 list the strongest flux density at $v = 1$ and $v = 2$, while columns 7 and 8 list the radial velocities at which each occurs. The position angle of the E vector of polarization for the observation is given in column 9. Pairs of numbers refer to separate $v = 1$ (first) and $v = 2$ (second) measurements. The integrated flux of the entire velocity range after a linear baseline was removed is given in columns 10 and 11. These columns and the distance from column 3 lead to the luminosities given in columns 12 and 13. The first published SiO maser reference for each star is listed in column 14 and the notes.

Negative results are listed in Table II, along with the integration time and spectrometer. AK/10 and AK/5 refer to the autocorrelator at bandwidths of 10 and 5 MHz; FISPE refers to the filter spectrometer. The 3σ noise limits are given for each of $v = 1$ and $v = 2$.

We searched 13 of the stars in Table I for $v = 3$ emission, finding it in the direction only of VX Sgr, as previously reported (Scalise and Lépine 1978), and VY CMa. The peak flux density and radial velocity of our detections are presented in Table III, as well as the 3σ noise limits in other stars.

IV. DISCUSSION

The high-resolution spectra of Figs. 1–8 represent the best basis for the study of SiO masers yet available. Forty-six of the approximately 75 stars known to have SiO masers are included in a homogeneous high-resolution study. This sample is large enough that the general properties of SiO maser emission can be studied without referring to the peculiarities of a single source or a small number of sources.

Of the 46 detected stars, 12 are identified in Table I as new detections at 7 mm: 11 masers associated with classical Mira variables and OH 26.5+0.6, the first Type II OH/IR source detected in any SiO line (OH detected at 1612, 1665, and 1667 by Andersson *et al.* 1974, H_2O detected by Olnon *et al.* 1980). RX Boo was previously

TABLE I. Positive results.

Star	IRC No.	Dist. (pc)	Phase	Strongest feature (Jy) $v=1$	(Jy) $v=2$	(km s^{-1}) $v=1$	(km s^{-1}) $v=2$	Pol. angle (deg)	Integrated flux ($\times 10^{-20}$ W m^{-2}) $v=1$	Integrated flux ($\times 10^{-20}$ W m^{-2}) $v=2$	Log luminosity (W) $v=1$	Log luminosity (W) $v=2$	Ref.
(1)	(2)	(3)	(4)	(5)	(6)	(7)	(8)	(9)	(10)	(11)	(12)	(13)	(14)
R Aqr	−20642	233	0.16[a]	270	95	−26	−26	−14	100 ± 20	40 ± 10	20.81	20.41	8
W Aqr	+00489	406[b]	0.90[a]	20	23	+1	+2	−13	15 ± 3	7 ± 5	20.46	20.15	1
R Aql	+10406	203	0.48[a]	17	20	+46	+46	−11	11 ± 5	2 ± 3	19.73	18.99	2
RR Aql	+00458	446	0.71[a]	91	56	29	29	−2	22 ± 5	10 ± 4	20.72	20.37	2
RT Aql	+10433	518	0.94[a]	37	14	−28	−26	9	12 ± 4	5 ± 3	20.58	20.20	7
GY Aql	−10524	582[b]		69	98	+30	+35	+14	41 ± 8	50 ± 10	21.23	21.30	5
V1300 Aql	−10529	620[d]	0.6[f]	32	40	−19	−20	−14	7 ± 6	14 ± 6	20.51	20.81	6
U Ari	+10040	531	0.21[a]	34	34	−57	−57	−4	7 ± 2	8 ± 4	20.37	20.43	1
RX Boo	+30257	563[b]	0.21	18	30	−1	+4	−19	9 ± 2	13 ± 3	20.53	20.69	3
R Cnc	+10185	296	0.44[a]	33	27	16	15	32	22 ± 4	7 ± 6	20.36	19.86	4, 6
VY CMa	−30087	1500[c]		600	580	13	13	−15	940 ± 190	390 ± 80	23.40	23.02	2
R Cas	+50484	182	0.9[a]	680	270	26	28	60	360 ± 70	180 ± 40	21.15	20.85	2
T Cas	+60009	239	0.7[a]	30	≤20	+1	—	26	3 ± 3	—	19.30	—	1
Y Cas	+60001	506	0.64[a]	15	21	−17	−17	−45	10 ± 5	7 ± 4	20.48	20.32	7
Z Cas	+60418	1202	0.21[a]	19	20	−28	−28	−45	10 ± 4	12 ± 4	21.23	21.32	1
T Cep	+70168	188	0.6[a]	64	≤24	−3	—	54	31 ± 5	—	20.11	—	4, 6
o Cet	+00030	90	0.72[a]	144	172	48	48	7	33 ± 6	33 ± 7	19.51	19.51	2
S CrB	+30272	366	0.35[a]	148	109	−1	−1	20, 33	27 ± 3	27 ± 5	20.65	20.65	2
UX Cyg	+30464	1180	0.37[a]	29	24	3	3	−47	16 ± 7	13 ± 4	21.43	21.34	7
χ Cyg	+30395	128[b]	0.70[a]	32	≤12	9	—	−15	9 ± 3	—	19.24	—	2
NML Cyg	+40448	500[d]		350	220	4	4	42, 5	140 ± 20	82 ± 10	21.62	21.38	2
U Her	+20298	316	0.66[a]	24	24	−16	−18	−21	10 ± 7	7 ± 6	20.08	19.92	2
RU Her	+30282	532	0.83[a]	61	49	−11	−11	−27	29 ± 6	26 ± 6	20.99	20.94	6
R Hya	−20254	131	0.2[a]	77	110	−10	−11	7	33 ± 10	40 ± 10	19.83	19.91	2
W Hya	−30207	288[b]		1180	680	41	41	5	610 ± 120	280 ± 60	21.78	21.45	2
X Hya		436	0.6[a]	16	18	26	27	−17	13 ± 7	18 ± 6	20.46	20.61	1
R Leo	+10215	244[b]	0.4[a]	330	270	4	1	−20	200 ± 40	150 ± 30	21.15	21.04	2
R LMi	+30215	300	0.16[a]	235	190	1	1	−47	90 ± 20	60 ± 10	20.99	20.81	4
GX Mon		1367[b]	0.19[a]	14	15	−7	−10	−20	5 ± 5	6 ± 6	21.04	21.03	1
V1111 Oph	+10365	500[d]		57	48	−30	−32	−36	34 ± 8	26 ± 8	21.00	20.89	5
S Ori	+00074	402	0.13[a]	59	51	15	13	−21	34 ± 8	13 ± 7	20.81	20.40	1
U Ori	+20127	267	0.68	34	22	−33	−31	−35	15 ± 6	7 ± 3	20.11	19.77	3
R Peg	+10527	411	0.14[a]	102	76	23	23	−26	70 ± 10	39 ± 7	21.15	20.90	4
W Peg		307	0.56[a]	18	27	−17	−17	−45	6 ± 3	8 ± 3	19.83	19.95	1
S Per	+60088	2250[e]		45	36	−43	−43	−31	30 ± 6	21 ± 4	22.26	22.10	3
WX Psc	+10011	510[d]	0.6[a]	70	75	8	8	−33	19 ± 5	24 ± 5	20.77	20.87	6
Z Pup	−20133	853	0.93[a]	55	≤30	+1	—	−2	18 ± 8	—	21.20	—	7
VX Sgr	−20431	500[d]		1590	850	4	3	2	1370 ± 270	710 ± 140	22.61	22.32	2
R Ser	+20285	382	0.69[a]	55	53	29	29	34	12 ± 3	11 ± 3	20.32	20.28	1
S Ser	+10290	767[b]	0.26[a]	29	≤18	29	—	35	10 ± 8	—	20.85	—	1
WX Ser	+20281	970[d]	0.05[a]	61	24	7	9	36	33 ± 9	14 ± 5	21.57	21.20	2
R Tau	+10060	421[b]	0.03[a]	32	28	13	14	16	9 ± 5	13 ± 5	20.28	20.43	8
IK Tau	+10050	284	0.1[a]	125	100	39	39	31	90 ± 20	80 ± 20	20.94	20.89	2
RS Vir	+00243	642[b]	0.1[a]	76	34	−14	−15	−23	17 ± 6	9 ± 5	20.92	20.64	1
RT Vir	+10262	1348[b]		25	≤22	13	—	−19	18 ± 5	—	21.59	—	4
OH 26.5+0.6		—	—	7	8	29	28	−13	1 ± 1	5 ± 2	—	—	1

[a] Included in statistical analysis.
[b] Distance determined from absolute magnitude from Foy *et al.* 1975 (see text).
[c] Distance from Herbig (1969).
[d] Distance from Hyland *et al.* (1972).
[e] Distance of h and χ Perseus clusters Allen (1973).
[f] Phase from Harvey *et al.* (1974).

References

1. This paper.
2. Snyder and Buhl (1975).
3. Kaifu, Buhl, and Snyder (1975).
4. Spencer *et al.* (1977).
5. Balister *et al.* (1977).
6. Blair and Dickinson (1977).
7. Dickinson *et al.* (1978b).
8. Lépine, Le Squeren, and Scalise (1978).

known as an 86-GHz SiO emitter (Kaifu, Buhl, and Snyder 1975).

Variation of SiO maser intensity similar to that reported for OH and H_2O masers has been reported (Spencer and Schwartz 1975; Hjalmarson and Olofsson 1979). The data are still too sparse for a meaningful analysis and, thus, we have not corrected our data for periodic variation of maser strength.

a) Velocities and Line Profiles

SiO maser emission is restricted to a small velocity

TABLE II. Negative results (3σ).

Star	Integration time (s)	Spectrometer	Flux density limit (Jy) $v=1$	Flux density limit (Jy) $v=2$	Star	Integration time (s)	Spectrometer	Flux density limit (Jy) $v=1$	Flux density limit (Jy) $v=2$
W And	294	AK/10	15.7	16.6	X Gem	588	AK/10	18.5	18.0
T Aqr	294	AK/10	22.9	22.7	BU Gem	294	AK/10	18.1	15.9
RV Aqr	294	AK/10	24.3	23.5	η Gem	294	AK/10	18.7	16.0
χ Aqr	294	AK/10	23.4	25.6	S Her	294	AK/10	14.7	15.8
W Aql	588	AK/10	16.5	16.8	S Her	233	FISPE	11.1	11.1
RS Aql	588	AK/10	18.5	16.7	T Her	588	AK/10	13.3	13.1
T Ari	294	AK/10	14.4	16.2	W Her	294	AK/10	18.9	17.9
R Aur	294	AK/10	19.3	19.3	W Her	233	FISPE	7.0	7.0
S Aur	294	AK/10	17.6	16.4	X Her	117	FISPE	9.5	9.5
U Aur	294	AK/10	15.2	14.8	RS Her	588	AK/10	12.2	11.6
RU Aur	294	AK/10	18.1	17.7	UV Her	294	AK/10	15.7	16.0
TU Aur	294	AK/10	15.9	12.9	UW Her	233	FISPE	17.1	17.1
UU Aur	298	AK/10	15.6	19.1	g Her	233	FISPE	5.4	5.4
UZ Aur	233	FISPE	6.6	6.6	S Hya	294	AK/10	19.7	20.8
R Boo	588	AK/10	12.0	12.3	T Hya	294	AK/10	24.7	24.7
S Boo	588	AK/10	13.9	15.6	U Hya	294	AK/10	24.3	22.3
V Boo	294	AK/10	21.7	19.7	V Hya	294	AK/10	28.6	28.6
W Boo	235	AK/10	15.4	18.4	RU Hya	294	AK/10	47.3	47.3
RV Boo	294	AK/10	17.9	22.1	S Lac	294	AK/10	15.9	18.6
RW Boo	294	AK/10	16.1	16.7	R Lyn	294	AK/10	15.6	15.6
VZ Cam	294	AK/10	14.5	12.2	R Lyr	280	FISPE	5.1	5.1
V Cnc	588	AK/10	18.2	18.4	W Lyr	294	AK/10	21.1	18.2
W Cnc	588	AK/10	16.3	15.9	V Mon	294	AK/10	22.1	21.8
X Cnc	294	AK/10	13.7	13.3	X Mon	294	AK/10	19.8	17.7
RS Cnc	294	AK/10	12.0	9.3	SY Mon	294	AK/10	19.3	20.2
R CVn	294	AK/10	15.7	15.6	CL Mon	294	AK/10	26.9	28.0
V CVn	294	AK/10	11.7	9.1	R Oph	294	AK/10	36.4	36.4
Y CVn	294	AK/10	11.7	13.0	X Oph	294	AK/10	24.5	26.1
S CMi	294	AK/10	22.8	26.0	Z Oph	294	AK/10	20.0	22.8
V CMi	294	AK/10	15.6	18.9	RT Oph	294	AK/10	19.8	19.3
S Cas	588	AK/10	12.8	13.3	X Ori	294	AK/10	23.6	24.1
U Cas	588	AK/10	14.4	15.2	α Ori	588	AK/10	32.3	—
V Cas	588	AK/10	17.0	16.1	S Peg	588	AK/10	15.3	16.8
SV Cas	588	AK/10	24.8	24.8	Z Peg	294	AK/10	17.8	15.9
PZ Cas	588	AK/10	16.2	18.5	UU Peg	294	AK/10	21.8	20.7
X Cep	294	AK/10	14.9	15.0	R Per	233	FISPE	9.6	9.6
μ Cep	294	AK/10	17.0	17.0	U Per	588	AK/10	16.4	17.6
R Cet	294	AK/10	27.3	23.6	RR Per	233	FISPE	11.7	11.7
R Com	588	AK/10	11.4	12.2	SU Per	233	FISPE	7.2	7.2
R CrB	59	AK/10	61.0	52.0	GI Per	294	AK/10	14.5	16.0
V CrB	233	FISPE	8.1	8.1	VZ Sge	294	AK/10	11.6	12.9
RR CrB	233	FISPE	5.4	5.4	RR Sco	353	AK/10	52.3	56.6
RS CrB	233	FISPE	5.6	5.6	BG Ser	294	AK/10	18.7	20.0
P Cyg	294	AK/10	12.9	12.9	Z Tau	294	AK/10	20.2	18.4
R Cyg	233	FISPE	5.1	5.1	RX Tau	294	AK/10	18.1	18.9
R Cyg	204	AK/10	15.8	14.6	CE Tau	233	FISPE	11.3	11.3
U Cyg	294	AK/10	11.9	12.8	R Tri	147	AK/10	19.9	20.6
V Cyg	294	AK/10	12.4	12.7	R UMa	294	AK/10	15.4	15.4
W Cyg	294	AK/10	11.3	11.9	S UMa	588	AK/10	16.8	17.2
Z Cyg	294	AK/10	11.9	12.8	T UMa	588	AK/10	11.5	11.6
RT Cyg	294	AK/10	15.4	14.1	Y UMa	353	AK/10	15.1	15.1
RU Cyg	294	AK/10	12.6	11.5	Z UMa	294	AK/10	10.8	13.5
RV Cyg	294	AK/10	12.0	12.9	ST UMa	294	AK/10	13.4	14.1
SX Cyg	294	AK/10	20.6	17.8	S UMi	294	AK/10	19.2	18.5
TT Cyg	294	AK/10	12.0	12.4	U UMi	588	AK/10	14.6	14.0
AF Cyg	233	FISPE	6.3	6.3	RR UMi	294	AK/10	15.6	15.6
CN Cyg	294	AK/10	14.3	16.0	R Vir	588	AK/10	14.7	14.4
V1057 Cyg	294	AK/10	16.2	15.1	S Vir	294	AK/10	22.9	23.9
R Del	294	AK/10	18.2	19.3	U Vir	294	AK/10	20.7	21.7
U Del	294	AK/10	16.9	16.9	RX Vul	294	AK/10	17.6	19.2
V Del	588	AK/10	11.6	12.9	IRC−10502	294	AK/10	23.3	26.1
R Dra	294	AK/10	21.9	22.1	IRC+00357	294	AK/10	26.7	23.7
T Dra	294	AK/10	33.7	26.3	IRC+00402	294	AK/10	24.0	27.8
RY Dra	294	AK/10	13.2	13.2	IRC+10216 (=CW Leo)	294	AK/10	20.4	19.5
UX Dra	233	FISPE	5.1	5.1					
R Gem	294	AK/10	19.0	19.0					

range. For the red giants, including NML Cyg, the emission is confined to a velocity spread of 7 to 15 km s^{-1}. The supergiants VY CMa, S Per, and VX Sgr show emission over about 30 km s^{-1}. One-half of these values (3.5 to 15 km s^{-1}) are reasonable velocities to associate with mass loss from late-type stars. The large range of

TABLE III. $v = 3$ results.

Star	Spectrometer	Peak flux density (Jy)	Radial velocity ($km\,s^{-1}$)
RX Boo	AK/10	<22	
VY CMa	AK/10	110 ± 22	41
R Cas	FISPE	<1.0	
NML Cyg	AK/10	<17	
NML Cyg	FISPE	<1.5	
χ Cyg	AK/10	<8	
χ Cyg	FISPE	<1.7	
U Her	FISPE	<1.0	
W Hya	AK/10	<12	
R Leo	AK/10	<26	
R LMi	AK/10	<11	
VX Sgr	AK/10	70 ± 14	4
RT Vir	AK/10	<22	
IRC+10216	AK/10	<18	

velocities covered by the FISPE observations (up to 140 $km\,s^{-1}$) would have been sufficient to detect emission similar to the high-velocity emission of water masers in some regions of star formation (Walker *et al.* 1977). At some velocities, not necessarily related to the stellar velocity, to the velocity of the optical emission, or to optical absorption, strong, narrow, SiO emission is observed. In the supergiants such as VY CMa or S Per there are more than two strong narrow peaks. If the $v = 1$ and $v = 2$ lines originated in the expanding stellar envelopes, there should be a correlation between the total width of the line profile and the period of the light variations (Dickinson and Chaisson 1973; Dickinson *et al.* 1978a). No such correlation was found, which indicates that these masers are situated close to the stars themselves.

The line profiles of the spectra range from simple to complex. With our higher sensitivity and resolution, the complexity of the spectra has increased relative to earlier observations. Earlier descriptions of *o* Cet and other stars as having double-peaked emission similar to OH masers are oversimplified. SiO maser spectra consist of many blended features that are frequently unresolved with the 0.2-$km\,s^{-1}$ resolution of some of the spectra in Figs. 1–8. Typical blended features appear to be 1 to 2 $km\,s^{-1}$ wide. In most sources only a few velocities are favored, and they dominate the spectra. The VLBI observations confirm this conclusion (Moran *et al.* 1979; Lane *et al.* 1980).

b) *Weak Satellite Emission*

Snyder *et al.* (1978) discovered a weak broad-line emission associated with the dominant narrow masers that had been previously studied. They referred to this emission as a "pedestal," and felt that the center velocity of the pedestal yields stellar radial velocities: The "pedestal represents a useful extension to the radial velocity method introduced by Reid and Dickinson (1976)."

We find that weak satellite maser emission (i.e., broad, blended emission often over a wide velocity range) is common in our larger sample of stars. This satellite maser emission is what Snyder *et al.* (1978) observed, but with their lower resolution and sensitivity the masers appeared to merge together into a broad feature. We cannot separate these weak satellites from the stronger lines as clearly as Snyder *et al.* (1978) have done. At the time of our observations there was no narrow emission for many stars and in most stars the strong emission lines blended into the weak satellite masers. It is often difficult to separate weak masers in the satellite region from stronger ones closer in with the high resolution and sensitivity of these spectra.

Snyder *et al.* (1978) removed the main-line emission, then fit a parabola to the quasi-thermal pedestal to obtain a stellar velocity. If we were to attempt this process on the present epoch spectrum of VY CMa, the center velocity would be in the range of 18 to 20 $km\,s^{-1}$ instead of the 13.1 ± 0.1 $km\,s^{-1}$ found by Snyder *et al.* (1978). The weaker system near 40 $km\,s^{-1}$, which includes a narrow maser feature and weak satellite masers, would indicate a second long-period variable star, in the analysis of Snyder *et al.* (1978), which is unlikely. Furthermore, $v = 1$ and $v = 2$ spectra for many of the stars with clear satellite emission yield different stellar velocities. The spectra of Figs. 1–8 indicate that weak maser emission can occur within a limited velocity range, that more masers (or stronger masers) tend to be at the central velocities, but that there is no obvious parabolic or Gaussian distribution of emission. In particular, the stars previously found to have pedestals, VY CMa, R Cas, *o* Cet, NML Cyg, W Hya, R Leo, VX Sgr, and IK Tau, appear not to have simple parabolic pedestals, but to have a blend of weak masers adjacent to the strong emission.

c) *Variability*

The observations between 9 and 17 May 1979 show significant variations in stars that were observed repeatedly, usually for pointing corrections. The data were too sparse, however, to distinguish between temporal intensity variations and polarization effects, owing to the differing position angle of the *E* vector during the observations. While intensity variations in these sources are well known on longer time scales, the SiO masers also are known to be strongly polarized in the $J = 2$–1 transition (Troland *et al.* 1979) and to have some linear polarization at $J = 1$–0 (Schwartz *et al.* 1977). The cause of the present variations is therefore uncertain.

Table II contains further evidence of the intensity variability of SiO masers. W And, R Aur, and S Vir would have been detected at 5, 10, and 8 times the noise level, respectively, if they were as strong as their previously reported flux density at the epoch of these observations (Blair and Dickinson 1977; Dickinson *et al.* 1978b; Lépine, Le Squeren, and Scalise 1978). A fourth known star not detected, RR Sco, was at low elevations and the 3σ limit of ~55 Jy is close to the previously re-

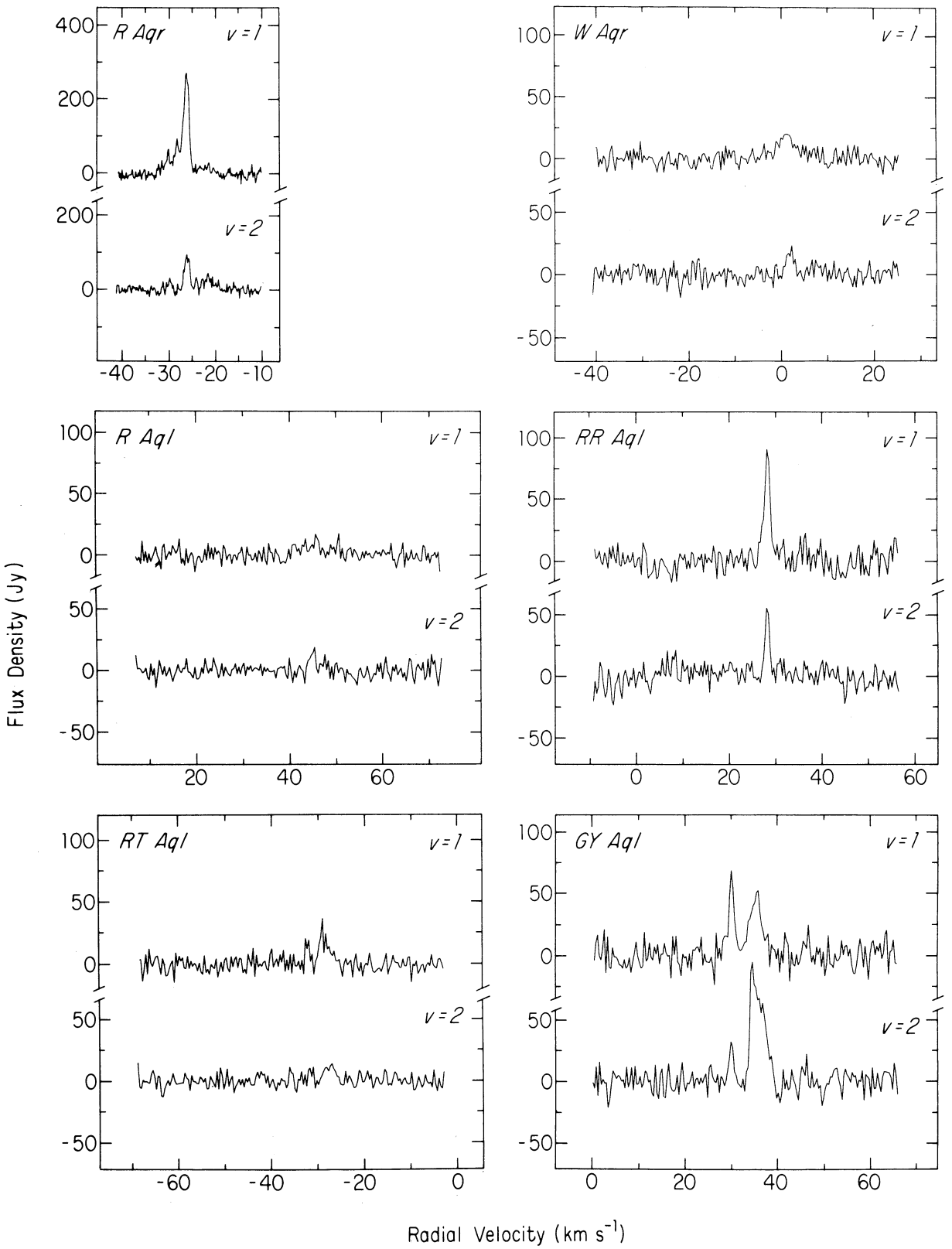

FIG. 1. $J = 1$–0, $v = 1$, and $v = 2$ SiO line profiles detected in the present work. Unless noted the spectrometer was either the AK/10 or AK/5 with uniform weighting. The two transitions are presented on the same flux density scale for each star. The radial velocities are relative to the local standard of rest.

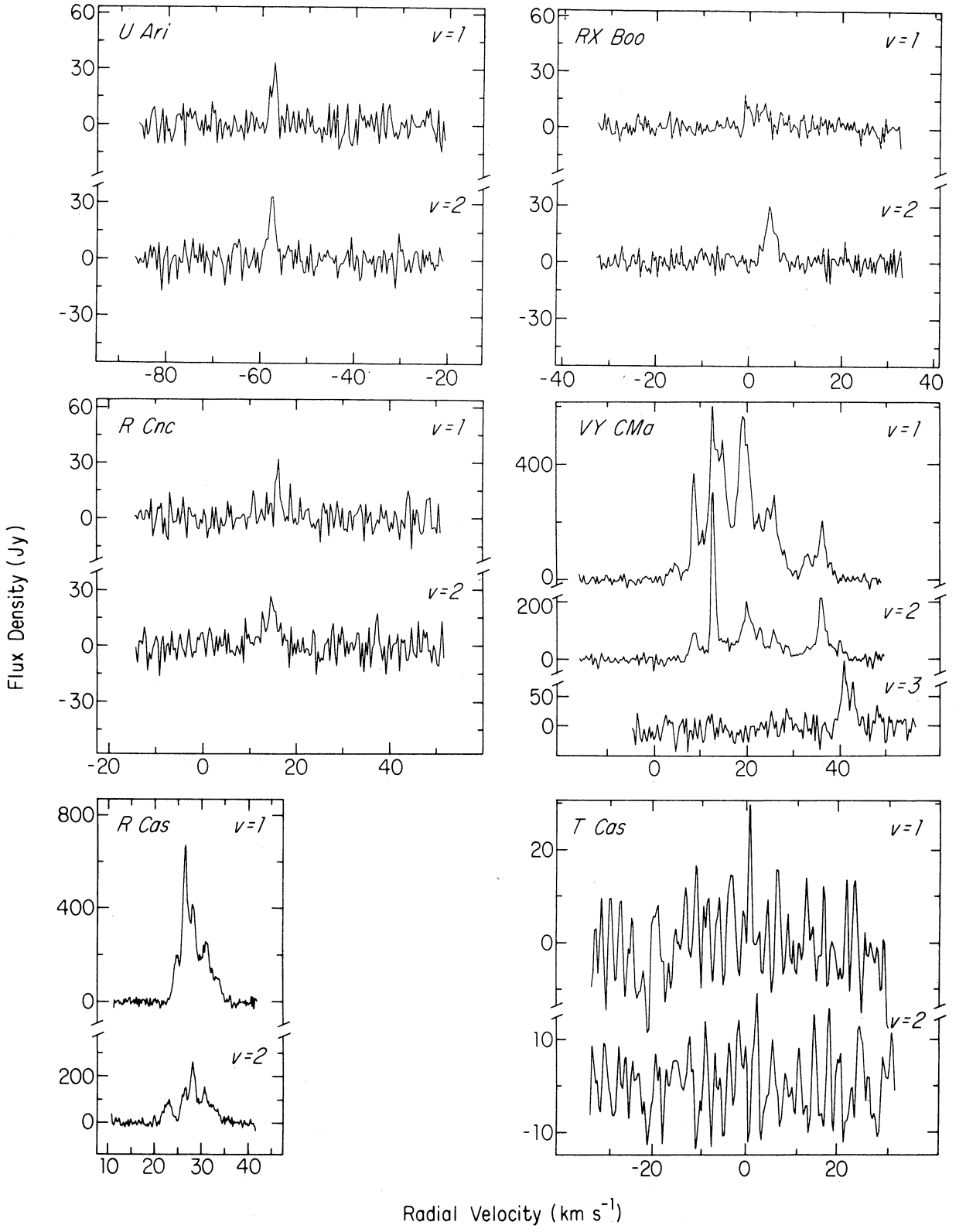

FIG. 2. Same as Fig. 1. Where $v = 3$ was detected (VY CMa) the flux density scale has been enlarged. The spectra for T Cas have been smoothed with Hanning weighting.

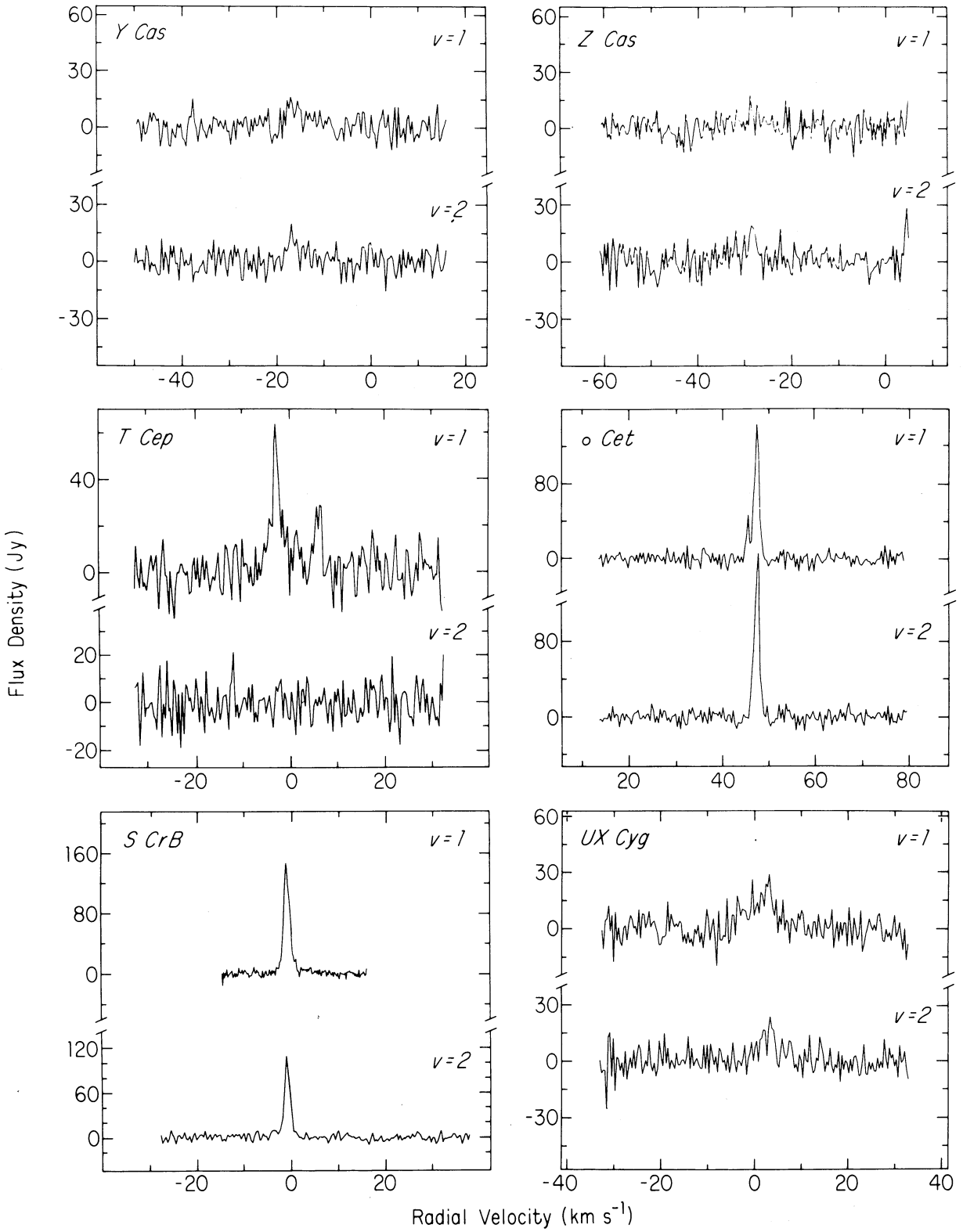

FIG. 3. Same as Fig. 1.

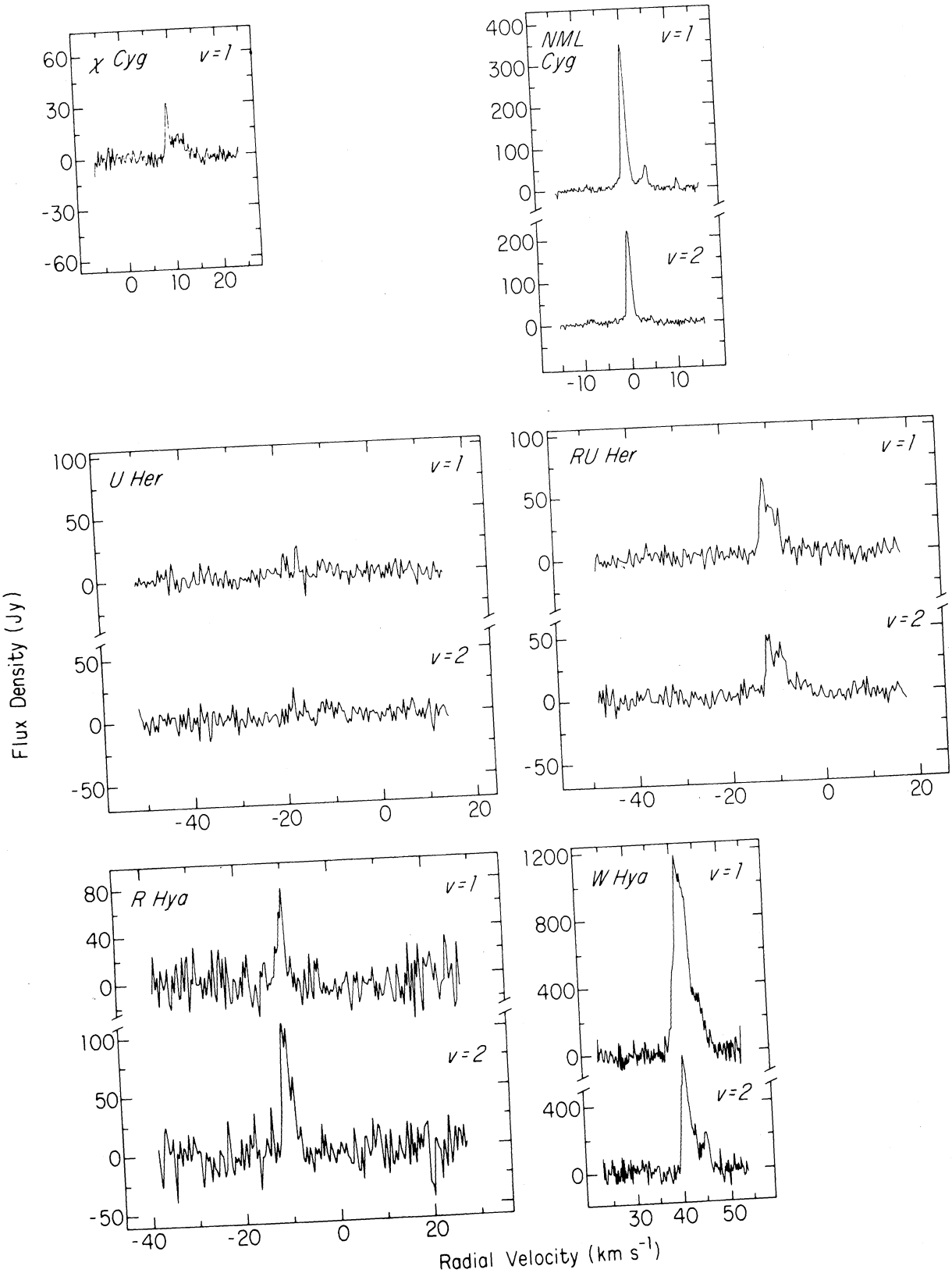

FIG. 4. Same as Fig. 1.

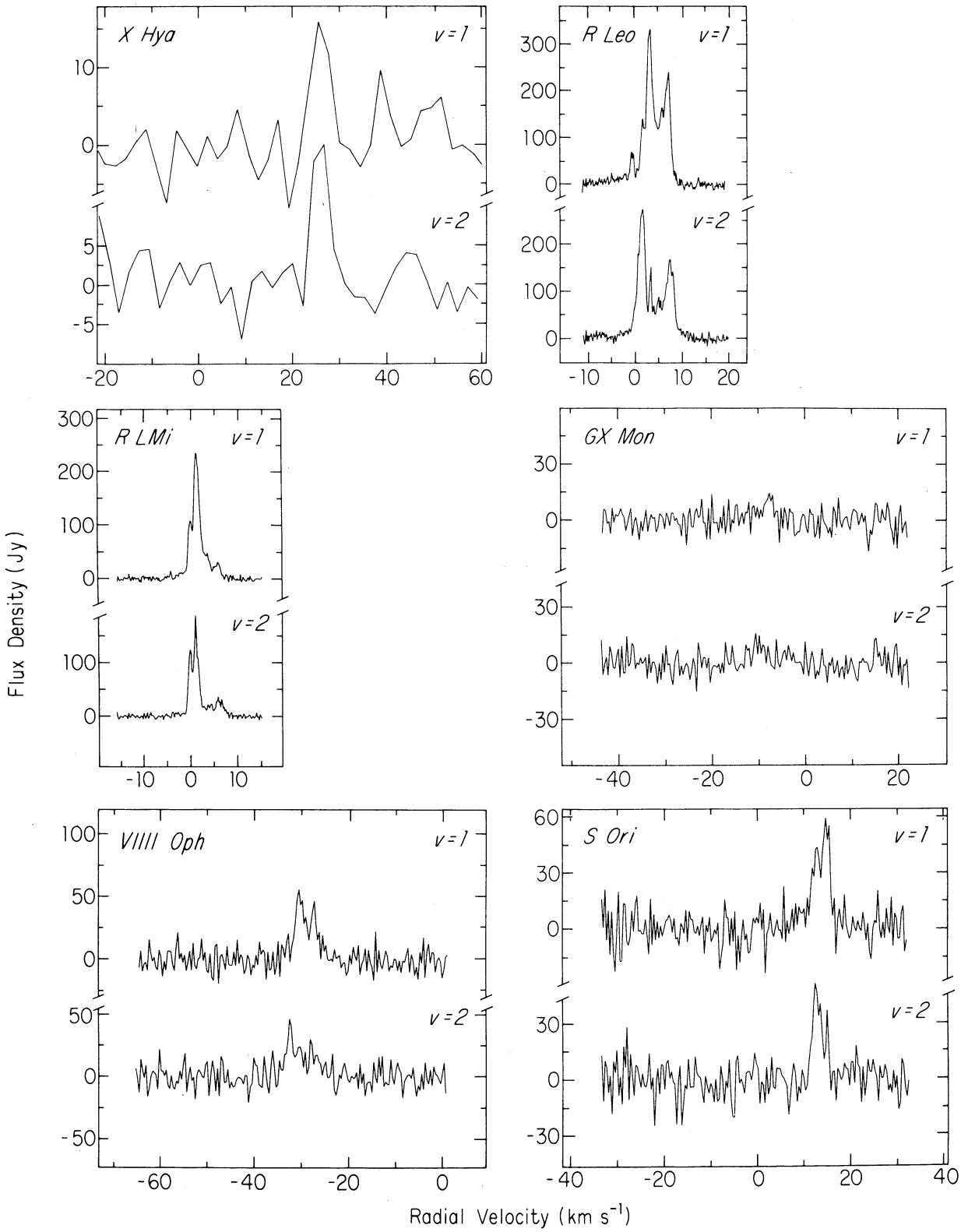

FIG. 5. Same as Fig. 1. The spectra for X Hya were taken with the FISPE spectrometer.

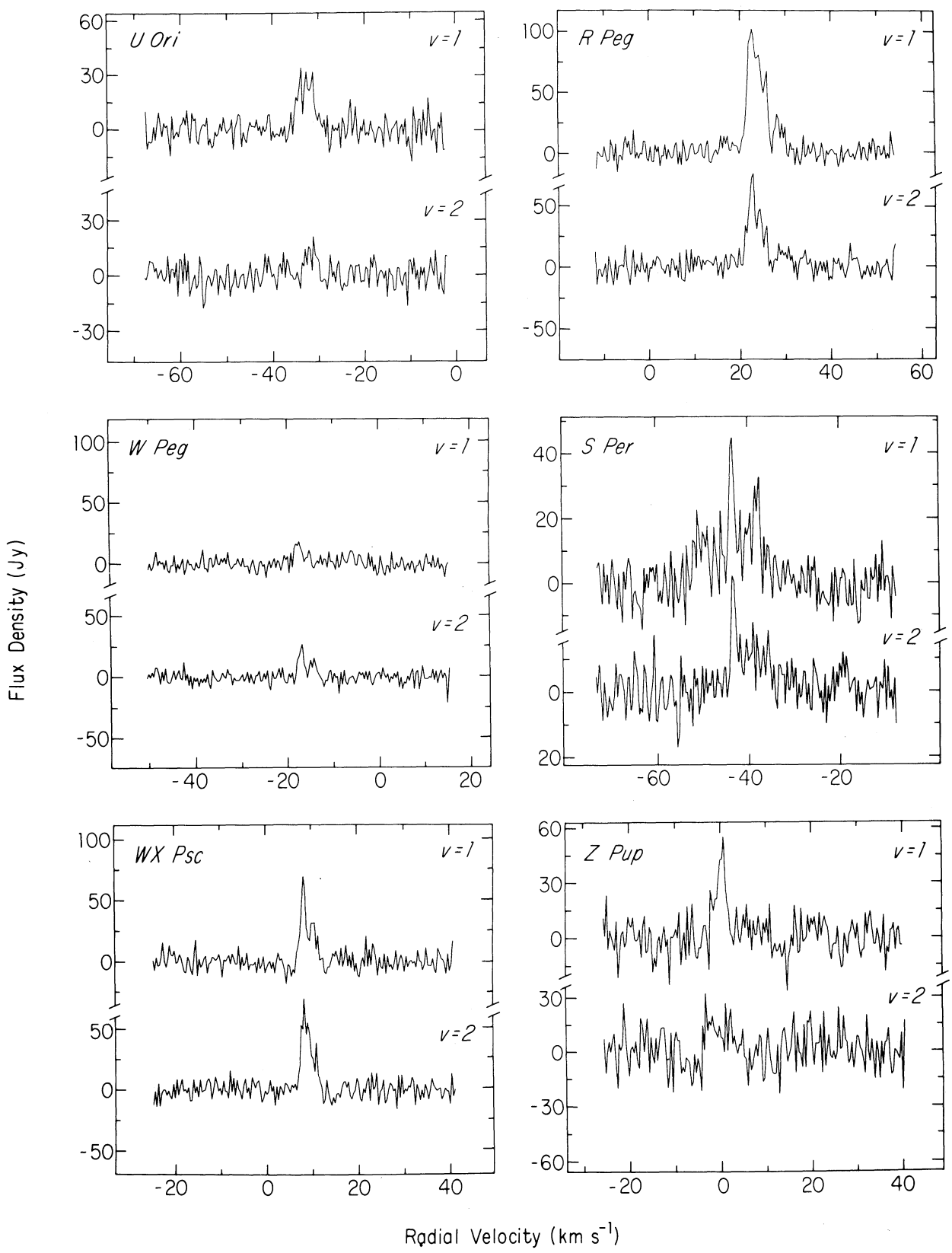

FIG. 6. Same as Fig. 1.

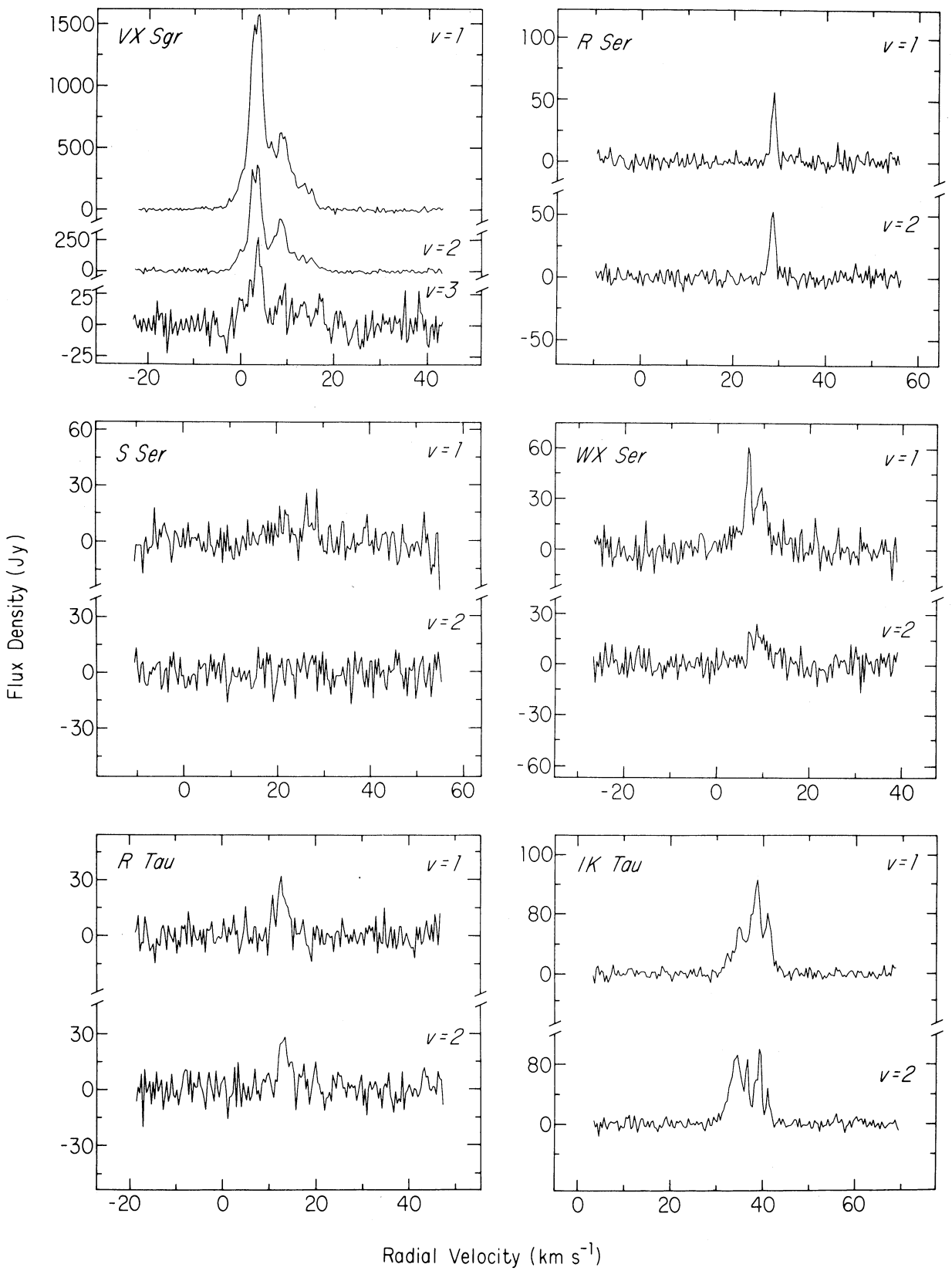

FIG. 7. Same as Fig. 1. Where $v = 3$ was detected (VX Sgr) the flux density scale has been enlarged.

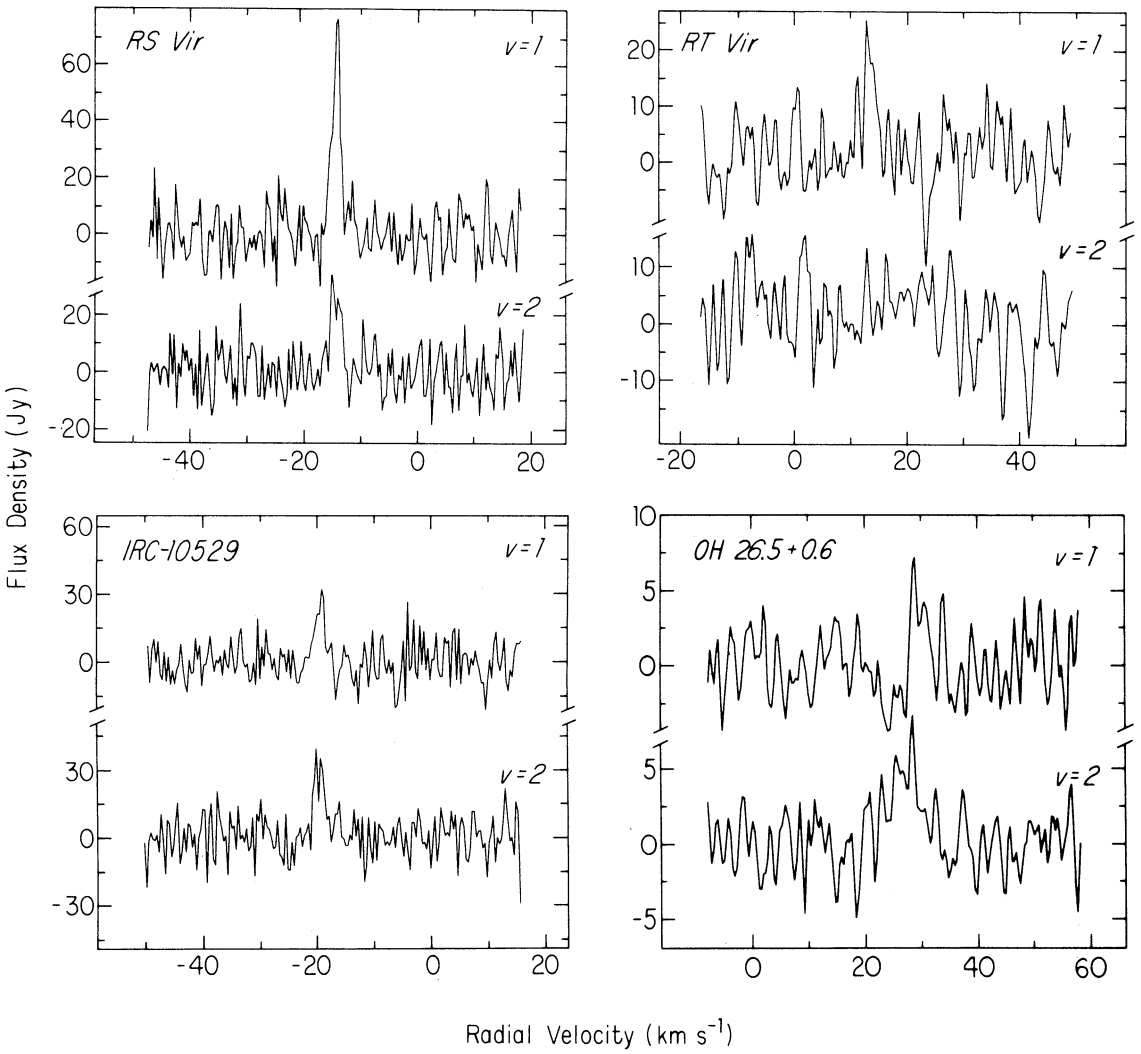

FIG. 8. Same as Fig. 1. The spectra for RT Vir and OH 26.5+0.6 have been smoothed with Hanning weighting.

ported $J = 2$–1 flux (Dickinson *et al.* 1978b). The $J = 1$–0 line has never been reported.

d) Sample Completeness

There are several methods that can be used to estimate the completeness of the sample. In a homogeneous, spherical distribution of maser stars, the log$N$-log$I$ relationship (Fig. 9) would have a slope of -1.5, where N is the total number of stars with an intensity greater than I. Clearly the total sample marked by the crosses in Fig. 9 is heterogeneous, possibly the cause of the complex shape of the curve. A more homogeneous sample, that of the 34 M-type Miras marked by footnote "a" in Table I, shows an underabundance below an intensity of $10^{-18.5}$ W m^{-2} owing to an incompleteness in the sample of masers. This flux corresponds to a distance limit of about 300 pc. Since the observations attempted to be complete to a greater distance, it appears these results are sensitivity limited. If the distribution of masers is not spherical, but confined to a thin disk, the slope of the log$N$-log$I$ relation would be -1. The late-type Miras in our sample have a scale height above the galactic plane of 165–300 pc (Smak 1966). Therefore we do not expect this to strongly affect our log$N$-log$I$ relation given the characteristic distance of completeness estimated above.

A second test for completeness is the luminosity-volume test (von Hoerner 1974). In this test one calculates the volume V of the sphere with a radius equal to the actual distance to the star divided by the volume V_m, corresponding to the maximum distance at which this particular star could have been detected. If the space distribution were uniform (and spherical), the frequency distribution of this function would be constant with a mean value of 0.5.

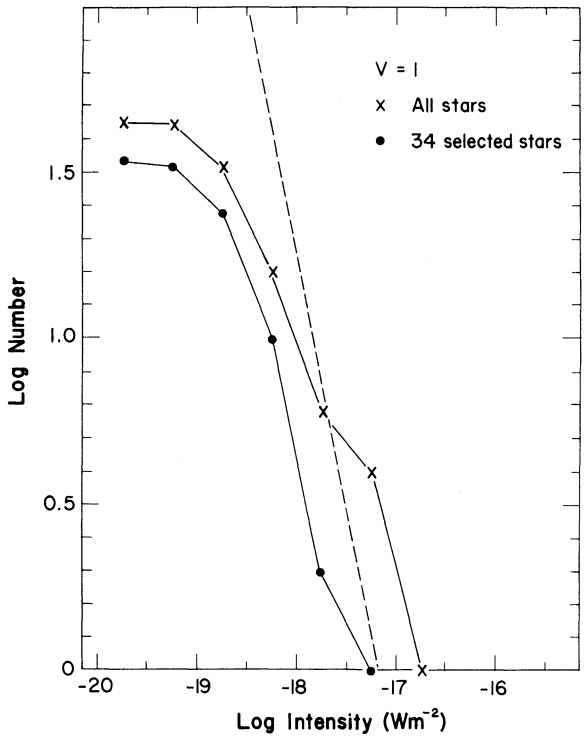

FIG. 9. The log$N$-log$I$ relation. The curve marked with x's includes all the stars in Table I. The curve marked with closed circles includes the 34 stars marked by a footnote "a" in Table I. The dashed line has a slope of −1.5, which one expects for a homogeneous, spherical distribution.

The quantity of interest, V/V_m, is equal to the signal-to-noise ratio to the −1.5 power and is independent of the assumed stellar distance. It is therefore strongly dependent on the detection criteria. We have calculated V/V_m using both flux density and integrated intensity separately. The resulting distributions are significantly weighted toward low values and exclude a mean value of 0.5. This supports the conclusion of the log$N$-log$I$ test that we are mainly dealing with nearby sources.

We made a third test for completeness, by projecting each detected star onto the galactic plane and counting the number of stars in heliocentric regions of equal areas. The radii were generated with the function

$$r_n^2 = r_{n-1}^2 + r_1^2, \qquad (2)$$

where we used $r_1 = 200$ pc. The results are presented in Table IV. If the stars were in a disk with uniform space density, then there would be an equal number in each interval. Once again we see problems in the distribution beyond a radius of ~300 pc.

If the noise in the spectra for all M-type Miras observed (positive and negative detections) is corrected to the stellar distance to get a peak luminosity limit, we get the distribution shown in Fig. 10. Peak luminosity is the luminosity per hertz that corresponds to the observed peak flux density. The numbers above each column show

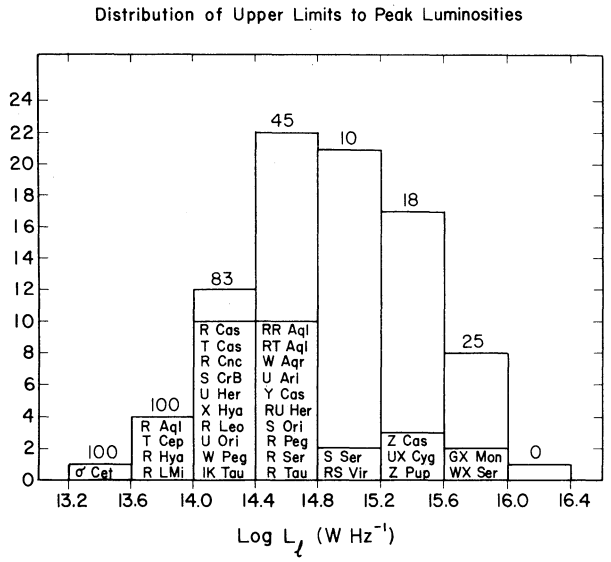

FIG. 10. The peak luminosity limits for all stars, both detected and undetected. The peak noise luminosity is the noise in an observed spectrum corrected to the stellar distance (see text).

the detection percentage. The negative results are predominantly at higher peak luminosity limits, again indicating that successful detections occurred for the closer stars. If the noise were to be reduced by an order of magnitude, through longer integration for instance, this figure predicts that the number of detected sources would double, but still there would be a number of negative results because of sensitivity limitations.

e) Luminosity Function

We would like to estimate the luminosity function of SiO masers. The luminosity distribution of the stars marked by footnote "a" in Table I is presented in Fig. 11. The mean luminosity based on Fig. 11 is 3.6×10^{20} W. The true luminosity function is expected to have more weak masers, decreasing this mean value.

We attempted to correct the observed luminosity distribution for incompleteness by using the upper limits for the undetected stars. This technique is applied on the peak luminosities and peak luminosity limits because the

TABLE IV. Equal surface test.

Radius from the Earth (pc)	Number of SiO maser stars in each area
0–200	7
200–283	8
283–346	2
346–400	5
400–447	2
447–490	1
490–529	2
529–566	0
566–600	1

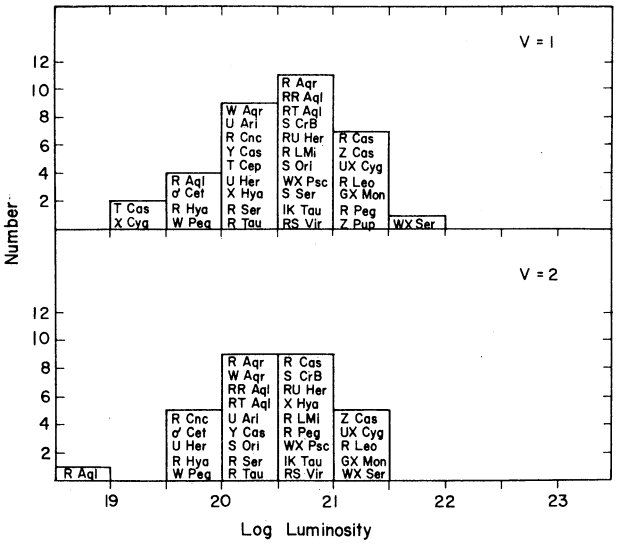

FIG. 11. The luminosity distribution for the stars with footnote "a" in Table I.

detection criteria were dominated by flux density deviations. Once a peak luminosity (W Hz^{-1}) is found, it can be converted to integrated luminosity by using linewidths.

Our method differs from that recently described by Avni *et al.* (1980). We use information of three types: detected luminosities, upper limits for nondetections, and equivalent noise limits for the detections. Their method uses only the first two types of information and requires slightly more mathematics. However, when we applied their technique to our data, the resultant luminosity functions were identical except for minor differences at low luminosities ($14 \lesssim \log L \lesssim 14.2$), where there is not much information.

Our procedure is first to convert the flux density limits for all objects (detected and undetected) to peak luminosity limits (the distribution shown in Fig. 10). Likewise, the peak flux densities of the detected objects are converted to peak luminosities. For every value of luminosity the stars with a luminosity limit less than or equal to that value are examined. We then calculate the fraction of stars with a peak luminosity greater than or equal to the test value, with respect to the total number of stars examined. These fractions are a function of luminosity. The complement is the cumulative luminosity distribution. The differential peak luminosity function is shown in Fig. 12, smoothed to 0.3 in log (W Hz^{-1}). The more luminous portion ($\log L_p > 15$) of the function is well defined, as confirmed by the observed luminosity distribution (the histogram in Fig. 12). For $\log L_p \lesssim 14.4$, large deviations from a smooth function would be expected because of the lack of information we have about masers with extremely low luminosity. While it is impossible to restore the luminosity function at low luminosities with the present sample, we believe that it is highly improbable that a significant fraction of Miras have $\log L_p < 14$. A power-law fit yields the relation $N \sim L_p^{-0.7}$ for $14.5 < \log L_p < 16$. This is half the slope found for OH maser emission from Type II OH/IR sources by Baud *et al.* (1980).

We are trying to find the SiO luminosity function and would like to describe its characteristics, not only over the range where it can be restored accurately, but also outside that range. At the high-luminosity end, we know that none of the ~85 stars has a $\log L_p$ larger than 15.8. The fitted power law, in contrast, has a fairly strong high-luminosity wing because of its low exponent. The power-law description must break down fairly soon above $\log L_p \sim 16$. Something similar happens at the low-luminosity side. We found 15 SiO emitters among

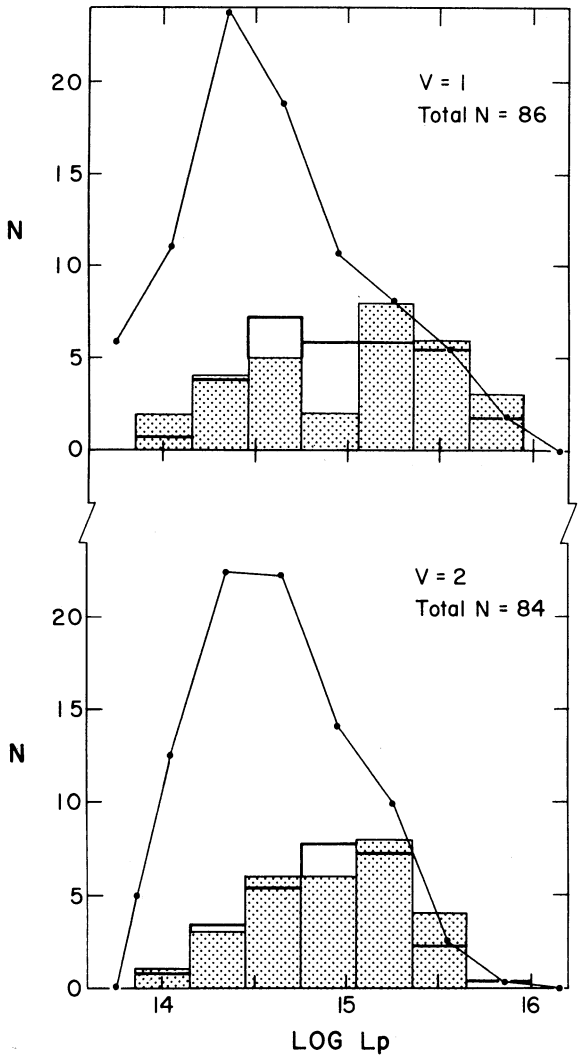

FIG. 12. The luminosity function for SiO masers found in Mira variables. This function is based on the observed distribution (shaded) and corrected for incompleteness, as described in the text. The predicted observed distribution is the bold histogram. (Upper) $v = 1$ luminosity function; (lower) $v = 2$ luminosity function.

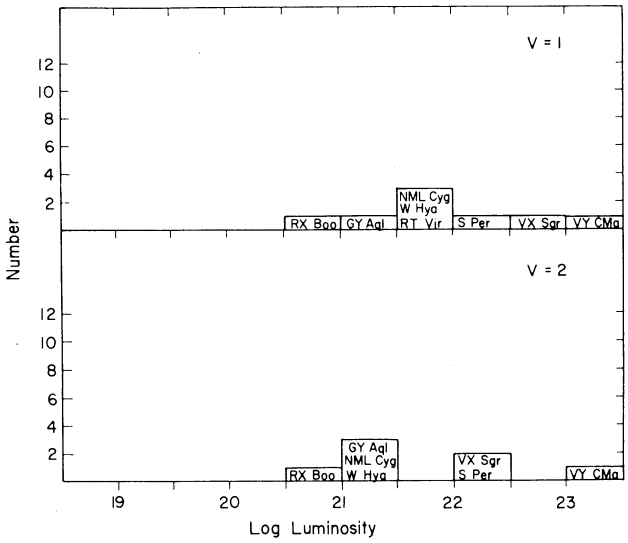

FIG. 13. The luminosity distribution for supergiant and semiregular stars listed in Table I.

the 17 stars with the lowest detection limits. That makes it highly improbable that a significant fraction of M-type Mira variables have $\log L_p$ below 14. Any power-law description of the luminosity function must break down below $\log L_p = 14.5$. Thus while $N \sim L_p^{-0.7}$ describes the luminosity function adequately over an important range, it is completely wrong outside that range. The SiO luminosity function (mean $\log L_p \sim 14.6$) is fairly narrow and extends over only two orders of magnitude.

The observed luminosity distribution of the masers associated with the supergiant and semiregular stars is shown in Fig. 13. As a class these masers are among the more luminous stellar masers. Even if the closer distance to VY CMa of 400 pc (Hyland *et al.* 1969) were adopted, it would still be the most luminous, with a luminosity of 1.8×10^{22} W. The OH and H_2O masers associated with this star are unusual for stellar masers. The individual H_2O masers in VY CMa are more compact, of smaller spot size, and more luminous than those in Mira variables (compare Rosen *et al.* 1978 with Spencer *et al.* 1979). The same is true for the OH masers (compare Reid and Muhleman 1978 with Bowers *et al.* 1980).

f) Correlations Among SiO Luminosity, Period, and Bolometric Luminosity

The $v = 1$ and $v = 2$ SiO luminosities were plotted versus stellar period, and no correlation was found. The scatter was fairly uniform over 300 to 450 days. For periods longer than 450 days, there seemed to be a deficiency of low-luminosity SiO masers, probably due to the method of selecting and observing these rarer stars.

The mean luminosity of the observed masers corresponds to an SiO maser flux of 2×10^{43} photons s^{-1}. This flux is about ten times the H_2O emission photon rate of about 2×10^{42} photons s^{-1} for these same stars. For Mira variables the number of photons at 4 μm available to pump the observed masers is about 10^{44} photons s^{-1}. If the SiO masers are radiatively pumped, it is reasonable to expect a correlation between SiO luminosity and stellar luminosity. Cahn and Elitzur (1979) found a correlation between SiO luminosity and the stellar luminosity at 4 μm. In the larger sample of masers presently available, there is no correlation between SiO luminosity and the total bolometric luminosity as derived from Cahn and Wyatt (1978). If we limit the stars to those in common with Cahn and Elitzur (1979), there is no correlation with 4 μm, contrary to their conclusion.

g) The Ratio of the v = 1 and v = 2 Line Intensities

A quantity which is distance independent is the ratio Q of the $v = 1$ to the $v = 2$ integrated intensities. The distribution of $\log Q$ is plotted in Fig. 14. For a Gaussian distribution, there is less than a 5% probability from the student's t test that the mean would be displaced from zero by chance. Thus we conclude that on the average the $v = 1$ line is 1.4 ± 0.1 times stronger than the $v = 2$ line in the same star.

This result may be compared with the average value $\overline{Q} = 0.95 \pm 0.50$ obtained for a sample of 13 stars and Orion in 1977 by Schwartz, Bologna, and Waak (1979). The two results are, within the errors, compatible.

If, according to Elitzur (1980), the SiO masers are in the stellar atmosphere and collisionally pumped, one would expect a correlation between Q and the effective temperature of the star because (again according to Elitzur) the densities in the atmospheres are about the same for all Miras. We find no such correlation nor any between Q and luminosity ($v = 1$) or Q and period.

h) The v = 3 Emission

Following the announcement of detection of $v = 3$ emission in W Hya and VX Sgr by Scalise and Lépine

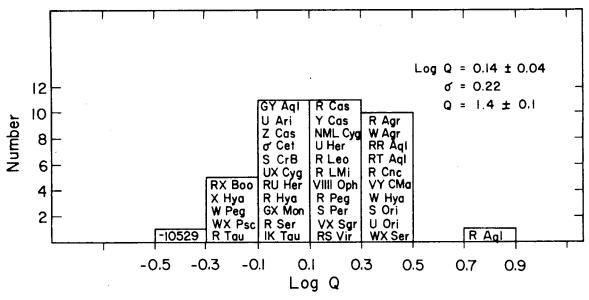

FIG. 14. The ratio of the $v = 1$ to the $v = 2$ integrated intensity (Q) for the stars with footnote "a" in Table I. The offset of $\log Q$ corresponds to a ratio of 1.4 ± 0.1.

(1978), we expected to confirm their sources and find new ones because we had a more sensitive system. As shown in Table III, this was not the case. We unexpectedly measured a 3σ rms upper limit in W Hya of 12 Jy, about one-third of the peak flux previously reported. This is much lower than the upper limit set by Buhl *et al.* (1974). Scalise and Lépine suggest that $v = 3$ emission is related to the light curve of the star. Our observational results neither support nor refute this hypothesis.

V. CONCLUSIONS

These observations, taken nearly simultaneously in the $v = 1$, $v = 2$, and $v = 3$ lines, greatly increase our data base for study of SiO maser emission. The high resolution and high sensitivity of these spectra show no evidence for "quasi-thermal pedestals" of emission, even though weak satellite masers are quite common. The main features are clearly blends of weak masers. There is a close velocity coincidence between line components in the $v = 1$ and $v = 2$ spectra of the same star. Only the velocity of $v = 3$ in VY CMa is highly anomalous. The SiO maser sample is now complete to approximately 300 pc, limited by sensitivity. We have detected 13 new sources. A luminosity function corrected for sample incompleteness has been derived and can be described as a power law with an exponent of -0.7. The luminosity functions are the same for $v = 1$ and $v = 2$, regardless of their true shapes. The $v = 1$ line is on the average 1.4 times stronger than the $v = 2$ line in the same star. No global properties of the stars correlate with the SiO luminosity, indicating that the masers are close to the stars, where local properties may be important. Yet the stellar temperature does not correlate with SiO luminosity. This complicates the situation and further understanding may require simultaneous observations at optical and infrared wavelengths and at 43- or 86-GHz SiO masers.

The authors would like to thank the many people at MPIfR who helped in these observations, especially the engineering and observing staffs. Our colleague V. Pankonin participated in the observations reported here and in their initial analysis. H.E.M. is grateful to the MPIfR for providing travel funds. We thank J. H. Cahn for providing distances to many of the Mira variables and S. von Hoerner for helpful discussions. A.W. was a guest of the National Radio Astronomy Observatory during the analysis of these data.

REFERENCES

Allen, C. W. (1973). *Astrophysical Quantities,* 3rd ed. (Athlone, London).
Altenhoff, W. J., Baars, J. W. M., Downes, D., Pankonin, V., Wink, J. E., Winnberg, A., Schwartz, P. R., Spencer, J. H., Matthews, H. E., Genzel, R., and Olnon, F. M. (1980). Astron. J. **85,** 9.
Andersson, C., Johansson, L. E. B., Goss, W. M., Winnberg, A., and Nguyen-Q-Rieu (1974). Astron. Astrophys. **30,** 475.
Avni, Y., Soltan, A., Tannanbaum, H., and Zamorani, G. (1980). Astrophys. J. **238,** 800.
Balister, M., Batchelor, R. A., Haynes, R. F., Knowles, S. H., McCulloch, M. G., Robinson, B. J., Wellington, K. J., and Yabsley, D. C. (1977). Mon. Not. R. Astron. Soc. **180,** 415.
Baud, B., Habing, H. J., Matthews, H. E., and Winnberg, A. (1980). Astron. Astrophys. (in press).
Blair, G. N., and Dickinson, D. F. (1977). Astrophys. J. **215,** 552.
Bowers, P. F., Reid, M. J., Johnston, K. J., Spencer, J. H., and Moran, J. M. (1980). Astrophys. J. **242** (in press).
Buhl, D., Snyder, L. E., Lovas, F. J., and Johnson, D. R. (1974). Astrophys. J. Lett. **192,** L97.
Cahn, J. H. (1980). Private communication.
Cahn, J. H., and Elitzur, M. (1979). Astrophys. J. **231,** 124.
Cahn, J. H., and Wyatt, S. P. (1978). Astrophys. J. **221,** 163.
Dickinson, D. F., and Chaisson, E. J. (1973). Astrophys. J. Lett. **181,** L135.
Dickinson, D. F., Reid, M. J., Morris, M., and Redman, R. (1978a). Astrophys. Lett. **220,** L113.
Dickinson, D. F., Snyder, L. E., Brown, L. W., and Buhl, D. (1978b). Astron. J. **83,** 36.
Elitzur, M. (1980). Astrophys. J. **240,** 553.
Engels, D. (1979). Astron. Astrophys. Suppl. **36,** 337.
Foy, R., Heck, A., and Mennessier, M. O. (1975). Astron. Astrophys. **43,** 175.
Genzel, R., Downes, D., Schwartz, P. R., Spencer, J. H., Pankonin, V., and Baars, J. W. M. (1980). Astrophys. J. **239,** 519.
Harvey, P. M., Bechis, K. P., Wilson, W. J., and Ball, J. A. (1974). Astrophys. J. Suppl. **27,** 331.
Herbig, G. H. (1969). Mem. Soc. R. Sci. Liege, Ser. 8, **13.**
Hjalmarson, A., and Olofsson, H. (1979). Astrophys. J. Lett. **234,** L199.
Hyland, A. R., Becklin, E. E., Frogel, J. A., and Neugebauer, G. (1972). Astron. Astrophys. **16,** 204.
Hyland, A. R., Becklin, E. E., Neugebauer, G., and Wallerstein, G. (1969). Astrophys. J. **158,** 619.
Kaifu, N., Buhl, D., and Snyder, L. E. (1975). Astrophys. J. **195,** 359.
Keenan, P. C., Garrison, R. F., and Deutsch, A. J. (1974). Astrophys. J. Suppl. **28,** 271.
Kleinmann, S. G., Dickinson, D. F., and Sargent, D. G. (1978). Astron. J. **83,** 1206.
Kukarkin, B. V., Kholopov, P. N., Efremov, Yu. N., Kukarkin, N. P., Kurochkin, N. E., Medvedeva, G. I., Perova, N. B., Fedorovich, V. P., and Frolov, M. S. (1969–1976). *General Catalog of Variable Stars,* 3rd ed. and supplements (Astronomical Council, Academy of Sciences, Moscow).
Lane, A. P., Ho, P. T. P., Predmore, C. R., Moran, J. M., Genzel, R., Hansen, S. S., and Reid, M. J. (1980). In *Interstellar Molecules,* IAU Symposium No. 87, edited by B. Andrew (Reidel, Dordrecht).
Lépine, J. R. D., Le Squeren, A. M., and Scalise, E., Jr. (1978). Astrophys. J. **225,** 869.
Low, F. J., Kurtz, R. F., Vrba, F. J., and Rieke, G. H. (1976). Astrophys. J. Lett. **206,** L153.
Moran, J. M., Ball, J. A., Predmore, C. R., Lane, A. P., Huguenin, G. R., Reid, M. J., and Hansen, S. S. (1979). Astrophys. J. Lett. **231,** L67.

Neugebauer, G., and Leighton, R. B. (1969). *Two-Micron Sky Survey,* NASA SP-3047 (U.S. GPO, Washington, D.C.).
Olnon, F. M., Winnberg, A., Matthews, H. E., and Shultz, G. V. (1980). Astron. Astrophys. Suppl. **42,** 119.
Reid, M. J., and Muhleman, D. O. (1978). Astrophys. J. **220,** 229.
Rosen, B. R., Moran, J. M., Reid, M. J., Walker, R. C., Burke, B. F., Johnston, K. J., and Spencer, J. H. (1978). Astrophys. J. **222,** 132.
Scalise, E., Jr., and Lépine, J. R. D. (1978). Astron. Astrophys. **65,** L7.
Schwartz, P. R., Bologna, J. M., and Waak, J. A. (1979). Astron. J. **84,** 1349.
Schwartz, P. R., Waak, J. A., Bologna, J. M., and Spencer, J. H. (1977). Bull. Am. Astron. Soc. **9,** 354.
Smak, J. I. (1966). Annu. Rev. Astron. Astrophys. **4,** 19.
Snyder, L. E., and Buhl, D. (1975). Astrophys. J. **197,** 329.
Snyder, L. E., Dickinson, D. F., Brown, L. W., and Buhl, D. (1978). Astrophys. J. **224,** 512.
Spencer, J. H., Johnston, K. J., Moran, J. M., Reid, M. J., and Walker, R. C. (1979). Astrophys. J. **230,** 449.
Spencer, J. H., and Schwartz, P. R. (1975). Astrophys. J. Lett. **199,** L111.
Spencer, J. H., Schwartz, P. R., Waak, J. A., and Bologna, J. M. (1977). Astron. J. **82,** 706.
Troland, T. H., Heiles, C., Johnson, D. R., and Clark, F. O. (1979). Astrophys. J. **232,** 143.
von Hoerner, S. (1974). In *Galactic and Extragalactic Radio Astronomy,* edited by G. L. Verschuur and K. I. Kellermann (Springer, New York), p. 353.
Walker, R. C., Johnston, K. J., Burke, B. F., and Spencer, J. H. (1977). Astrophys. J. Lett. **211,** L135.